

## A NEW MECHANICS MODEL OF STAMPING A THIN STRIP ON AN ELASTIC FOUNDATION

LIANGCHI ZHANG AND ZHONGQIN LIN\*

Center for Advanced Materials Technology, Department of Mechanical and Mechatronic Engineering, The University of Sydney, NSW 2006, Australia

(Received 17 June 1995; in revised form 6 December 1995)

**Abstract**—This paper proposes a new mechanics model and a semi-analytical method to solve the problem of a thin strip on an elastic foundation stamped by an elliptical rigid punch. The strip was divided into three parts according to its contact with the punch and foundation. Analytical solutions were derived individually for each part using the theories of contact mechanics and strip bending with large deflection. A numerical algorithm was then developed to obtain the interface forces through an iteration by considering the compatibility conditions of deformation between the neighbouring parts of the strip. The main advantages of the present method are that it relies on fewer assumptions, is with clear mechanics meaning throughout the analysis, and makes the calculation more efficient. Copyright © 1996 Elsevier Science Ltd.

### NOTATION

$a, b$	half lengths of the minor and major axes of the ellipse-based cylindrical punch, see Fig. 1
$c$	half length of the contact zone between the punch and strip
$c'$	half length of the contact zone between the strip and foundation
$E$	Young's modulus
$F$	external stamping force per unit width
$h$	thickness of the strip
$I$	the second moment of area per unit width of the strip cross section = $h^3/12$
$k_d$	elastic stiffness of the elastic foundation
$m$	dimensionless bending moment, defined by eqn (10)
$n$	dimensionless shear force, defined by eqn (10)
$q$	contact stress
$r$	dimensionless normal radius of ellipse, defined by eqn (9) (see also Fig. 4)
$ds$	dimensionless length of an infinitesimal strip element, defined by eqn (9) (see also Fig. 4)
$t$	dimensionless membrane force of the strip, defined by eqn (10)
$w$	deflection of the foundation surface, in the $y$ -direction
$w'$	deflection of the cantilever beam, vertical to the $z$ -axis, see Fig. 2(c)
$x, y$	global Cartesian coordinate system, defined by eqn (9), (see also Figs 2(a) and 3)
$z$	local axial coordinate of the cantilever beam, with its origin at end $A$ , see Fig. 2(c)
$\gamma, \eta$	computational parameters, defined by eqn (11)
$\theta$	polar coordinate variable of ellipse, see Fig. 3
$\phi$	included angle of the external normal of the deformed strip surface at $\theta$ with the positive direction of $y$ -axis, see Fig. 3
$\varphi$	included angle of the tangent of the deformed strip surface at $\theta$ with the positive direction of $x$ -axis, see Fig. 3
$\kappa$	curvature of the strip

### Subscripts

$c$	cantilever beam
$d$	elastic foundation
$e$	elastic limit
$n$	normal direction
$p$	punch
$t$	tangential direction
$0$	central point
$1$	contact-off point

\* On leave from Shanghai Jiao Tong University, Department of Mechanical Engineering.

## 1. INTRODUCTION

Stamping a thin strip on an elastic foundation by a rigid indenter is a mechanics problem commonly encountered in various engineering fields and has been studied extensively for some decades. However, the topic is still challenging because it poses a three-body contact problem involving the determination of the interface stress distributions between the strip and punch, and the strip and elastic foundation. The deformation of the system involves strong non-linearity associated with the interaction of the membrane force and bending moment.

A number of parametric studies have been carried out to understand the combined effect of plate and foundation properties through the modelling of plate deformation (Geiger, 1991; Low, 1981; Neumeister, 1992; Ratwani, 1973; Sankar, 1983; Ye, 1994; Zhang, 1995) and to provide a refined analysis of elastic foundation (Dempsey, 1991; Fan, 1994; Razaqpur and Shan, 1991; Girija, 1991). Nevertheless, the solution has not been very satisfactory because of the following problems:

(1) If an analytical approach is used, the distributions of the interface contact stresses are assumed *a priori* (e.g., Zhang, 1995), which limits the applicability of the solutions in terms of the indenter profiles, the ratio of the thickness of strip to punch radius, and the variation of the material properties of the strip and elastic foundation.

(2) A pure numerical analysis (e.g., Geiger, 1991) needs a considerable computational effort for the study of each specific case.

Accordingly, the development of a practical mechanics model and a corresponding solution method is of great importance. This paper proposes a new mechanics model to study the deformation mechanisms of a thin strip stamped by a rigid elliptical punch on an elastic foundation. Based on this, a semi-analytical method is generated to calculate the interface forces.

## 2. THE MECHANICS MODEL

Consider the stamping of a thin strip (thickness:  $h$ ) on an elastic foundation by a rigid ellipse-based cylindrical punch (half lengths of the minor and major axes:  $a$ ,  $b$ ). The deformation of the strip is in plane stress and is symmetrical to its central line, as shown in Fig. 1. The contact zones and interface stresses between the punch and strip and the strip and foundation are unknown in advance, which are functions of the punch stroke in the stamping process. Because of the symmetry of deformation, however, we can study half of the strip only. In order to analyse the problem properly, let us divide the strip into three parts according to its contact with the punch and elastic foundation (Fig. 2(a)): (1) the central part  $A'A$ , where the strip is in perfect contact with both the punch and foundation surfaces, (2) the transition part  $AC$ , where the strip is in perfect contact with the foundation but has no contact with the punch, and (3) the free part  $CD$ , where no contact takes place with either the punch or foundation.

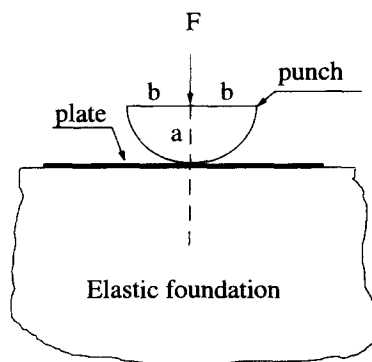


Fig. 1. Stamping a strip on an elastic foundation.

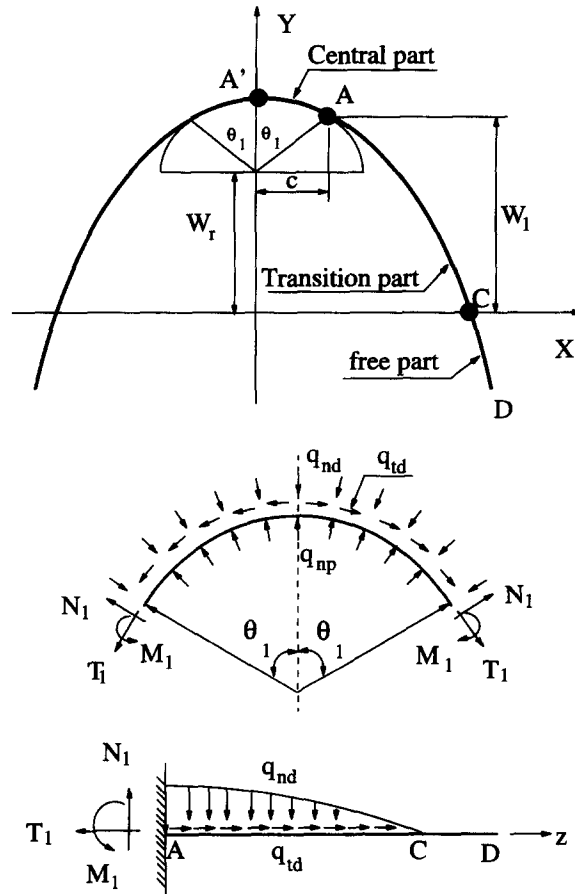


Fig. 2. The mechanics model.

The curvature of the central part is a known function which is identical to that of the punch surface. The contact stresses on the strip of this part are the normal contact stresses between the strip and punch,  $q_{np}$  and  $q_{ip}$ , and the normal and tangential ones between the strip and elastic foundation,  $q_{nd}$  and  $q_{td}$ . However,  $q_{ip}$  is negligible compared with  $q_{td}$ . Thus, we will ignore it in the following analysis, see Fig. 2(b).

The transition part can be modelled as a cantilever beam subjected to both normal and tangential stresses,  $q_{nd}$  and  $q_{td}$ , due to the interaction between the strip and foundation, see Fig. 2(c). The end  $A$  of this part is the contact-off point between the punch and strip, and end  $C$  is the contact-off point between the strip and elastic foundation. The boundary conditions of the cantilever must be specified to guarantee the continuity of stresses and deformation across these two ends, i.e.,

- (a) The bending moment, membrane and shear force are zero at  $C$ .
- (b) The deflection and its slope, bending moment and membrane force are equal to those of the central part at  $A$ .

The free part of the strip,  $CD$ , does not deform during stamping. Its displacement relies on the deflection and deflection slope at end  $C$ , and can be calculated easily when the solution to  $AC$  is obtained. Hence, we will ignore this part in the following analysis.

To simplify the calculation of the contact stresses, we assume that the normal reaction of the elastic foundation follows the Winkler's hypotheses, and that the tangential contact stress between the strip and foundation is proportional to the normal stress, i.e.,  $q_{td} = \mu q_{nd}$ , where  $\mu$  is the friction coefficient. In the next section, we will first obtain the analytical solutions to parts  $A'A$  and  $AC$ , and then calculate stresses using a numerical scheme in conjunction with the compatibility conditions of deformation between the two parts.

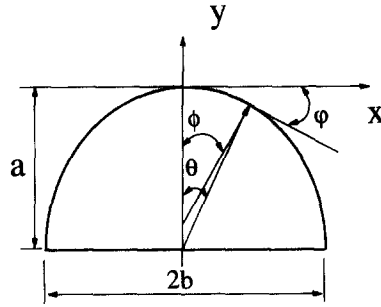


Fig. 3. The elliptical punch.

3. SOLUTIONS

3.1. Mathematical description of the mechanics model

The equations of strip bending of large deflection can be expressed as (Yu and Zhang, 1996)

$$\frac{dX}{dS} = \cos \phi, \quad \frac{dY}{dS} = \sin \phi, \quad \frac{d\phi}{dS} = \frac{M}{E_s I} = \kappa, \tag{1}$$

where  $X$  and  $Y$  are Cartesian coordinates,  $\phi$  is the included angle of the tangent of the deformed strip surface at  $\theta$  with the positive direction of  $X$ -axis (Fig. 3),  $dS$  is the length of an infinitesimal strip element (Fig. 4),  $E_s$  is Young's modulus of the strip material,  $I$  is the second moment of area per unit width of the strip cross section,  $\kappa$  is the curvature, and  $M$  is the bending moment. The equilibrium equation of the strip with large deflection can be written as

$$\begin{cases} \frac{dT}{d\phi} + N + RQ_t = 0, \\ \frac{dN}{d\phi} - T + RQ_n = 0, \\ \frac{dM}{d\phi} - RN = 0, \end{cases} \tag{2}$$

where  $T$  is the membrane force,  $N$  is the shear force,  $Q_n$  and  $Q_t$  are normal and tangential stresses,  $\phi$  is the included angle of the external normal of the deformed strip surface at  $\theta$  with the positive direction of the  $Y$ -axis, and  $R$  is the curvature radius of strip, see Figs 3 and 4. According to the assumption of Winkler's foundation, we have

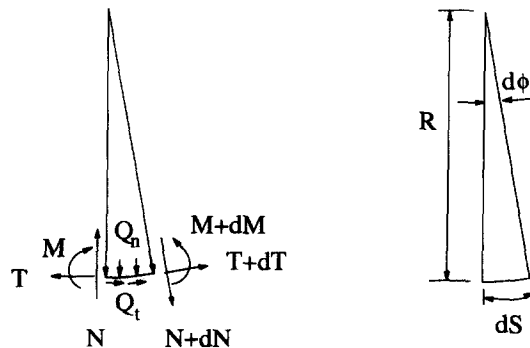


Fig. 4. A strip element in equilibrium.

$$Q_{nd} = k_d W, \quad Q_{td} = \mu k_d W, \quad (3)$$

where  $k_d$  is the stiffness coefficient of the elastic foundation,  $\mu$  is the friction coefficient between the strip and elastic foundation,  $W$  is the surface deflection of the foundation, and  $Q_{nd}$  and  $Q_{td}$  are the normal and tangential contact stresses between the strip and foundation. Furthermore, the compatibility conditions between parts  $A'A$  and  $AC$  can be expressed as

$$M(\theta_1^-) = M(\theta_1^+), \quad T(\theta_1^-) = T(\theta_1^+), \quad W(\theta_1^-) = W(\theta_1^+), \quad \varphi(\theta_1^-) = \varphi(\theta_1^+), \quad (4)$$

where  $\theta_1$  is the polar coordinate at the contact-off section  $A$ , with the superscripts ‘-’ and ‘+’ indicating parts  $A'A$  and  $AC$ , respectively. The compatibility conditions state that the deflection of the strip is a continuous function of  $C^2$ . Equations (1)–(4) can also be written in non-dimensional forms to generalise the solutions:

$$\frac{dx}{ds} = \cos \varphi, \quad \frac{dy}{ds} = \sin \varphi, \quad \frac{d\varphi}{ds} = \eta_1 m = \frac{1}{r}, \quad (5)$$

$$\begin{cases} \frac{dt}{d\phi} + n + \gamma_2 r q_t = 0, \\ \frac{dn}{d\phi} - t + \gamma_2 r q_n = 0, \\ \frac{dm}{d\phi} - 6\gamma_2 r n = 0, \end{cases} \quad (6)$$

$$q_{nd} = \eta_2 w, \quad q_{td} = \mu \eta_2 w, \quad (7)$$

$$w(\theta_1^-) = w(\theta_1^+), \quad \varphi(\theta_1^-) = \varphi(\theta_1^+), \quad m(\theta_1^-) = m(\theta_1^+), \quad t(\theta_1^-) = t(\theta_1^+), \quad (8)$$

where

$$x = \frac{X}{\sqrt{ab}}, \quad y = \frac{Y}{\sqrt{ab}}, \quad r = \frac{R}{\sqrt{ab}}, \quad ds = \frac{dS}{\sqrt{ab}}, \quad w = \frac{W}{a}, \quad (9)$$

$$M_e = \frac{1}{6} \sigma_y h^2, \quad N_e = \sigma_y h, \quad T_e = \sigma_y h, \quad k_e = \frac{E_d}{2a},$$

$$m = \frac{M}{M_e}, \quad n = \frac{N}{N_e}, \quad t = \frac{T}{T_e}, \quad q = \frac{Q}{\sigma_y}, \quad (10)$$

$$\gamma_1 = \frac{b}{a}, \quad \gamma_2 = \frac{\sqrt{ab}}{h}, \quad \eta_1 = \frac{2\sigma_y \sqrt{ab}}{E_s h}, \quad \eta_2 = \frac{E_d \sqrt{a}}{2\sigma_y \sqrt{b}},$$

$$\eta_3 = \frac{a^2 E_d}{2bh\sigma_y}, \quad \eta_4 = \frac{hbE_s}{2a^2 \sigma_y}, \quad \eta_5 = \frac{bh^2 E_s}{4a^3 \sigma_y}, \quad \eta_6 = \frac{h^2 b^2 E_s}{24a^4 \sigma_y}, \quad (11)$$

where  $\sigma_y$  is the yield stress and  $E_d$  is Young’s modulus of the elastic foundation.

### 3.2. Solution to part $A'A$

The deformation of the strip in this zone follows exactly the geometrical profile of the punch. Therefore, using the geometrical equation of an ellipse, the deflection function of the strip can be written as (see Fig. 4)

$$x = \sqrt{\gamma_1} \sin \theta, \quad y = \frac{1}{\sqrt{\gamma_1}} [\cos \theta - 1], \quad r = \frac{1}{\sqrt{\gamma_1^3}} \sqrt{(\sin^2 \theta + \gamma_1^2 \cos^2 \theta)^3}, \quad (12)$$

$$w = (w_r + \cos \theta - 1), \quad w_r = (1 - \cos \theta_1 + w_1), \quad (13)$$

where  $w_r$  is the punch displacement at the punch centre,  $w_1$  is the displacement at the contact-off point  $A$ , see Fig. 2(a). The bending moment and shear force in the strip can easily be determined when eqn (12) is substituted into eqns (5) and (6):

$$m(\theta) = \frac{\eta_3}{\sqrt{(\sin^2 \theta + \gamma_1^2 \cos^2 \theta)^3}}, \quad m(\theta_1^-) = \frac{\eta_3}{\sqrt{(\sin^2 \theta_1 + \gamma_1^2 \cos^2 \theta_1)^3}}, \quad (14)$$

$$n(\theta) = \frac{dm}{d\theta} \frac{d\theta}{d\phi} \frac{1}{6\gamma_2 r} = \frac{-\eta_4(1 - \gamma_1^2) \cos \theta \sin \theta}{(\sin^2 \theta + \gamma_1^2 \cos^2 \theta)^3}, \quad (15)$$

where the relationship between  $\theta$  and  $\phi$  is shown in Section A.1 of the Appendix. Using eqns (7) and (13), the contact stresses between the strip and elastic foundation can be expressed as

$$q_{nd} = \eta_2(w_1 - \cos \theta_1 + \cos \theta), \quad q_{td} = \mu\eta_2(w_1 - \cos \theta_1 + \cos \theta). \quad (16)$$

Accordingly, the membrane force of the strip and the normal contact stress between the punch and strip are

$$\begin{aligned} t(\theta) &= t_0 - \int_0^\theta n \frac{d\phi}{d\xi} d\xi - \int_0^\theta \gamma_2 r q_{td} d\xi \\ &= t_0 + \eta_5 \left[ \frac{1}{\gamma_1^6} - \frac{1}{(\sin^2 \theta + \gamma_1^2 \cos^2 \theta)^3} \right] - \eta_6 \mu [(w_1 - \cos \theta_1)G_1 + G_2] \end{aligned} \quad (17)$$

and

$$q_n = q_{np} - q_{nd}, \quad q_{np} = q_{nd} + \left( t - \frac{dn}{d\theta} \frac{d\theta}{d\phi} \right) \frac{1}{\gamma_2 r}, \quad (18)$$

when eqns (15) and (16) are substituted into eqn (6). In the above expressions,

$$G_1 = \int_0^\theta \sqrt{(\sin^2 \xi + \gamma_1^2 \cos^2 \xi)} d\xi, \quad G_2 = \int_0^\theta \cos \xi \sqrt{(\sin^2 \xi + \gamma_1^2 \cos^2 \xi)} d\xi, \quad (19)$$

$$\frac{dn}{d\theta} = -\eta_4(1 - \gamma_1^2) \frac{\cos 2\theta(\sin^2 \theta + \gamma_1^2 \cos^2 \theta) - 6(1 - \gamma_1^2) \cos^2 \theta \sin^2 \theta}{(\sin^2 \theta + \gamma_1^2 \cos^2 \theta)^4} \quad (20)$$

and  $t_0$  is the dimensionless membrane force at the central section  $A'$  of the strip. The calculation of  $G_1$  and  $G_2$  above is shown in Section A.4.1 of the Appendix.

### 3.3. Solution to part AC

As shown in Fig 2(a) and (c), the distributed load of this part is related to both the displacement at the contact-off section  $A$  and the deformation of the beam itself. Hence, according to eqn (7), the loads on the beam can be expressed as

$$q_{nc} = \eta_2 w = \eta_2 \left[ w_1 \left( 1 - \frac{z}{L} \right) - w' \cos \phi_1 \right], \quad q_{tc} = \mu q_{nc}, \quad 0 \leq z \leq L' \quad (21)$$

where  $\phi_1$  is the  $\phi$  value at section  $A$ ,  $w'$  is the deflection of cantilever beam which is in the same direction of punch normal at point  $A$ , as shown Fig. 2(a),  $L$  is the length of part  $AC$  when ignoring its deformation and  $L'$  is its length after deformation. In eqn (21), the first term in the square brackets is the surface deflection of the foundation when part  $AC$  is rigid, and the second term is caused by the deflection of  $AC$ . Consequently, the bending moment and membrane force can be expressed as

$$m = \int_z^{L'} \int_\xi^{L'} q_{nc} d\xi d\psi = \int_z^{L'} \int_\xi^{L'} \eta_2 \left[ w_1 \left( 1 - \frac{\psi}{L} \right) - w' \cos \phi_1 \right] d\psi d\xi,$$

$$m(\theta_1^+) = \int_0^{L'} \int_\xi^{L'} \eta_2 \left[ w_1 \left( 1 - \frac{\psi}{L} \right) - w' \cos \phi_1 \right] d\psi d\xi, \quad (22)$$

$$t = \int_z^{L'} q_{tc} d\xi = \int_z^{L'} \mu \eta_2 \left[ \frac{w_1}{L} (L - \xi) - w' \cos \phi_1 \right] d\xi,$$

$$t(\theta_1^+) = \int_0^{L'} \mu \eta_2 \left[ \frac{w_1}{L} (L - \xi) - w' \cos \phi_1 \right] d\xi, \quad (23)$$

where

$$w' = \int_z^{L'} \frac{\sin \varphi}{\cos \varphi} d\xi. \quad (24)$$

#### 3.4. Iteration technique

$w_1$  and  $t_0$  in the solutions of parts  $A'A$  and  $AC$  must be determined by the compatibility conditions. To simplify the procedure, we start the iteration by ignoring the deformation of part  $AC$ . A simple algorithm can be specified as follows:

- (i) give contact-off angle  $\theta_1$ ,
- (ii) calculate the internal forces of part  $AC$  by ignoring its deformation (see Section A.3 of the Appendix for further details), i.e.,

$$q_{nc} = \eta_2 w_1 \left( 1 - \frac{z}{L} \right), \quad q_{tc} = \mu q_{nc}, \quad L = \frac{w_1}{\sin \phi_1} \quad (25)$$

$$m = \int_z^L \int_\xi^L q_{nc} d\psi d\xi = \frac{\eta_2 w_1 L^2}{6} \left( 1 - \frac{z}{L} \right)^3, \quad m(\theta_1^+) = \frac{\eta_2 w_1^3}{6 \sin^2 \phi_1}, \quad (26)$$

$$t = \int_z^L q_{tc} d\xi = \frac{\mu \eta_2 w_1 L}{2} \left( 1 - \frac{z}{L} \right)^2, \quad t(\theta_1^+) = \frac{\mu \eta_2 w_1^2}{2 \sin \phi_1}, \quad (27)$$

- (iii) determine  $w_1^{(0)}, t_0^{(0)}$  with the compatibility conditions by eqns (14), (15), (26) and (27)

$$w_1^{(0)} = \sqrt[3]{\frac{6\eta_3\gamma_1^3 \sin^2 \theta_1}{\eta_2 \sqrt{(\sin^2 \theta_1 + \gamma_1^2 \cos^2 \theta_1)^3}}}, \quad (28)$$

$$t_0^{(0)} = \frac{\mu\eta_2 w_1^2}{2 \sin \phi_1} - \eta_5 \left[ \frac{1}{\gamma_1^6} - \frac{1}{(\sin^2 \theta_1 + \gamma_1^2 \cos^2 \theta_1)^3} \right] + \eta_6 \mu [(w_r - \cos \theta_1)G_1 - G_2], \quad (29)$$

- (iv) calculate the deflection of part  $AC$ , see Section A.2 of the Appendix,  
 (v) determine instant contact-off point  $C$  where  $q_{nc}^{(i)} = 0$ , and then calculate  $L'$ ,  
 (vi) correct the internal forces of part  $AC$ ,  $m$  and  $t$ , using

$$q_{nc}^{(i)} = \eta_2 \left[ w_1^{(i)} \left( 1 - \frac{z}{L} \right) - (w')^{(i)} \cos \phi_1 \right], \quad q_{ct}^{(i)} = \mu q_{cn}^{(i)}, \quad 0 \leq z \leq L', \quad (30)$$

which gives rise to

$$\begin{aligned} m(\theta_1^+) &= \int_0^{L'} \int_{\xi}^{L'} \eta_2 \left[ w_1^{(i)} \left( 1 - \frac{\psi}{L} \right) - w^{(i)} \right] d\psi d\xi, \\ t(\theta_1^+) &= \int_0^{L'} \mu \eta_2 \left[ w_1^{(i)} \left( 1 - \frac{\xi}{L} \right) - w^{(i)} \right] d\xi, \end{aligned} \quad (31)$$

- (vii) calculate  $w_1^{(i+1)}$  using the compatibility conditions, eqns (14), (15) and (33); here an internal iteration must be conducted until the compatibility conditions are all satisfied,  
 (viii) check the convergence according to criterion

$$\left| \frac{w_1^{(i+1)} - w_1^{(i)}}{w_1^{(i)}} \right| = \varepsilon, \quad (32)$$

where  $\varepsilon$  is a small positive constant; if it is satisfied, do the next step, otherwise, return to step (iv),

- (ix) calculate  $q_{mp}$ ,  $q_{nd}$ ,  $q_{td}$ ,  $t$ ,  $n$  and  $m$ .

#### 4. A NUMERICAL EXAMPLE

The numerical results presented in this section were calculated on a 486DX33 PC using the above algorithm. A complete analysis needs 10 minutes of computational time. Unless particularly specified, the material properties and geometrical dimensions used are  $E_s/E_d = 100$ ,  $a/h = 50$ ,  $E_s/\sigma_y = 875$ ,  $h = 1.0$  and  $\sigma_y = 240$  (MPa).

The distribution of the normal contact stress between the strip and punch is shown in Fig. 5, which demonstrates that the maximum stress moves from the centre towards the edge of the contact zone as  $\gamma_1$  increased. It is not difficult to understand that when  $\gamma_1$  increases the surface of the punch becomes more flat, and therefore a stress peak near the edge of the contact zone must appear. This is similar to the case of stamping with a flat punch. However, when  $\gamma_1 = 1$  (i.e., the punch profile is circular), the maximum contact stress will always be at the strip centre, as shown in Fig. 6.

Figure 7 compares the distributions of the normal contact stress between the punch and strip and that between the strip and elastic foundation. It is clear that the contact length between the punch and strip,  $c$ , and that between the strip and foundation,  $c'$ , are different and vary during stamping. When the contact angle  $\theta$  increases,  $c'$  approaches  $c$ . However, as the punch is rigid,  $c'$  is always larger than  $c$ . The softer the foundation, the larger the ratio of  $c'$  to  $c$ .

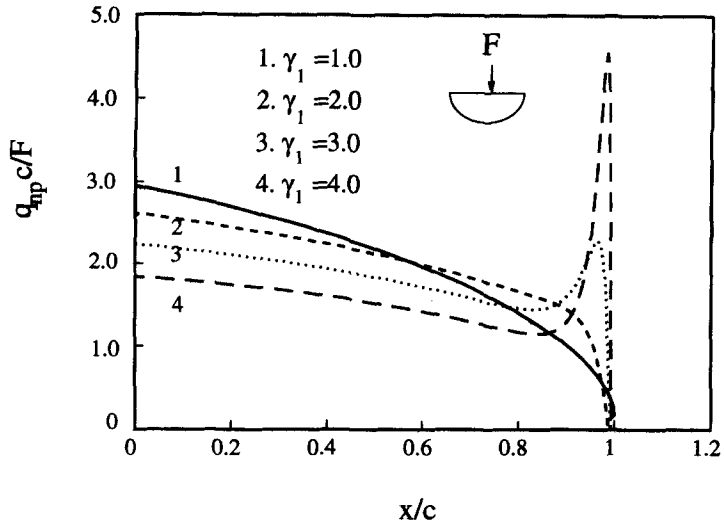


Fig. 5. The variation of the normal contact stresses between the punch and strip ( $\theta_1 = 90^\circ$ ).

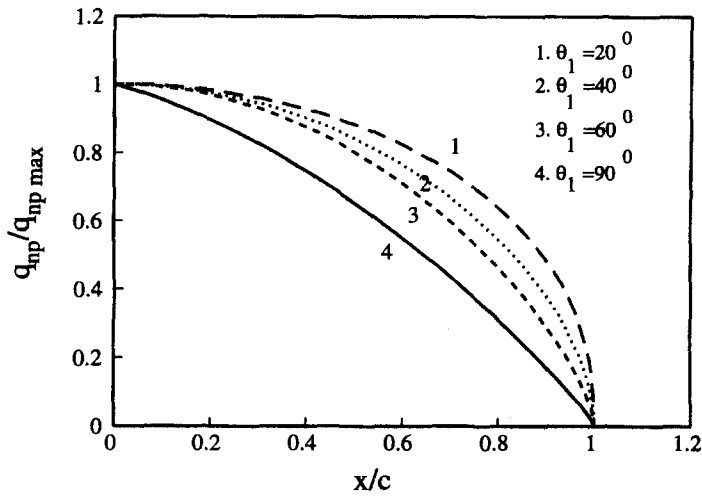


Fig. 6. The normal contact stresses between the punch and strip when  $\gamma_1 = 1$ .

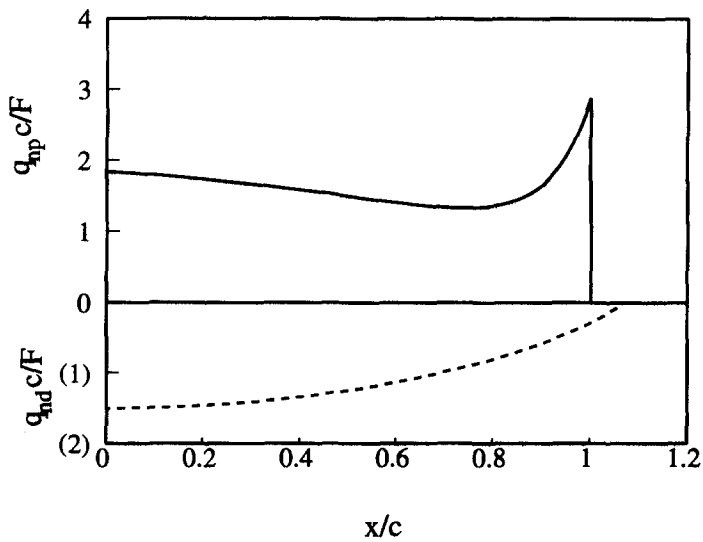


Fig. 7. The difference of the normal contact stresses on the lower and upper surfaces of the strip ( $\gamma_1 = 4.0, \theta_1 = 45^\circ$ ).

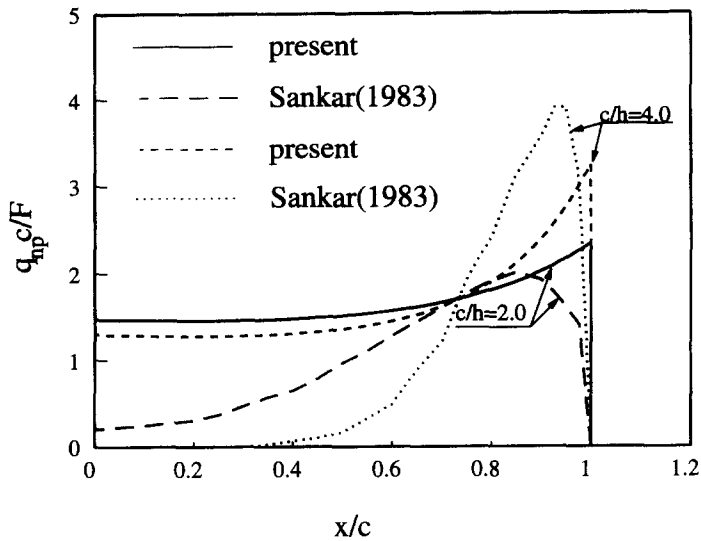


Fig. 8. The difference between stamping with and without a foundation ( $E_s/E_d = 1000$ ,  $a/h = 10$ ).

In a blank stamping process\*, a central gap appears between the punch and strip surfaces when the punch displacement reaches a certain value (Sankar, 1983; Yu and Zhang, 1996). Therefore, the contact force in this central zone must be zero. However, our extensive analyses indicate that for the stamping with an elastic foundation, such central separation does not happen, even when the foundation is very soft. Figure 8 is an example that demonstrates clearly the difference of contact stress distributions between these stamping processes.

Corresponding to the variation of the contact stresses, the internal forces of the strip,  $m$  and  $n$ , vary significantly with the elliptical ratio  $\gamma_1$ . When  $\gamma_1 = 1$ , the bending moment of the strip in part  $A'A$  is constant and the shear force is zero. This indicates a pure bending. When  $\gamma_1 < 1$ , the maximum bending moment is always at the strip centre. When  $\gamma_1 > 1$ , however, the maximum bending moment is always at the edge of part  $A'A$ . On the other hand, the general feature of the membrane force is that its peak moves from the centre towards the edge of the contact region with increasing  $\gamma_1$ . Recalling the effect of  $\gamma_1$  on the distribution of contact stresses discussed before, it is clear that  $\gamma_1$  is one of the most important geometrical parameters in stamping.

## 5. CONCLUSIONS

(1) The main advantages of the present model are that it relies on fewer assumptions, is with clear mechanics meaning throughout the analysis, and makes the calculation more efficient.

(2) The model and method developed can be extended easily to solve the problems of stamping with indenters of different geometries.

*Acknowledgements*—This work is supported by Australian Research Council through its small research grant scheme.

## REFERENCES

- Dempsey, J. P., Zhao, Z. G. and Li, H. (1991) Axisymmetric indentation of an elastic layer supported by a Winkler Foundation. *Int. J. Solids Structures* **27**, 73–87.
- Fan, H. and Keer, L. M. (1994). Two-dimensional contact on an anisotropic elastic half-space. *J. Appl. Mech.* **61**, 250–255.
- Geiger, M., Engel, U. and Ende, A. vom (1991). Investigations on the sheet bending process with elastic tools. *J. Materials Processing Tech.* **27**, 265–277.

\* The strip is simply supported at its ends.

- Ghani, Razaqpur A. and Shan, K. R. (1991) Exact analysis of beams on two-parameter elastic foundations. *Int. J. Solids Structures* **27**, 435–454.
- Giriya, Vallabhan C. V. and Das, Y. C. (1991). A refined model for beams on elastic foundations. *Int. J. Solids Structures* **27**, 629–637.
- Low, H. Y. (1981). Behaviour of a rigid-plastic beam loaded to finite deflections by a rigid circular indenter. *Int. J. Mech. Sci.* **23**, 387–393.
- Neumeister, J. M. (1992). On the role of elastic constants in multiphase contact problems. *J. Appl. Mech. Trans. ASME* **59**, 328–334.
- Ratwani, M. and Erdogan, F. (1973). On the plane contact problem for a frictionless elastic layer. *Int. J. Solids Structures* **9**, 921–936.
- Sanker, B. V. and Sun, C. T. (1983). Indentation of a beam by a rigid cylinder. *Int. J. Mech. Sci.* **19**, 293–303.
- Ye, Jianqiao (1994). An alternative approach for large deflection analysis of axisymmetric strips on elastic foundation. *Comm. Num. Meth. Engng* **10**, 623–632.
- Yu, T. X. and Zhang, L. C. (1996). *Plastic Bending: Theory and Application*, World Scientific, Singapore.
- Zhang, L. C. (1995). A mechanical model for sheet metal stamping by deformable dies. *J. Mat. Processing Tech.* **53**, 798–810.

## APPENDIX

### A.1. The relationship between $\theta$ and $\phi$

The tangent and normal of an ellipse can be expressed as

$$\begin{aligned} y_1 &= -\frac{x}{\gamma_1} \tan \theta + C_1 \quad (\text{tangent}), \\ y_2 &= \gamma_1 x \cot \theta + C_2 \quad (\text{normal}). \end{aligned} \quad (\text{A.1})$$

Therefore, according to Fig. 3,

$$\begin{aligned} \tan \phi &= \frac{\tan \theta}{\gamma_1}, \quad \frac{d\phi}{d\theta} = \frac{\gamma_1}{\sin^2 \theta + \gamma_1^2 \cos^2 \theta}, \\ \cos^2 \phi &= \frac{\gamma_1^2 \cos^2 \theta}{\sin^2 \theta + \gamma_1^2 \cos^2 \theta}, \quad \frac{d\theta}{d\phi} = \frac{(\sin^2 \theta + \gamma_1^2 \cos^2 \theta)}{\gamma_1}. \end{aligned} \quad (\text{A.2})$$

### A.2. Some detailed formula derivation for part AC

According to the basic equations of plate bending subjected to large deflection, the deflection of part AC can be expressed as

$$w' = \int_z^L \frac{\sin \phi}{\cos \phi} d\xi, \quad (\text{A.3})$$

where  $L'$  is the length of part AC, see Fig. 2(a) and (c). In order to solve eqn (A.3), it is necessary to find the relationship between the axial coordinate  $z$  and the slope of the deformed plate surface. Generally, the bending moment can be expressed as

$$m = \int_z^L \int_\xi^L \eta_2 \left[ w_1 \left( 1 - \frac{\psi}{L} \right) - w' \cos \phi_1 \right] d\psi d\xi. \quad (\text{A.4})$$

Substituting (A.4) into the geometrical equation of plate bending gives rise to

$$\frac{d\phi}{dz} = \frac{\eta_1 m}{\cos \phi} = \frac{\eta_1 \eta_2}{\cos \phi} \int_z^L \int_\xi^L \left[ w_1 \left( 1 - \frac{\psi}{L} \right) - w' \cos \phi_1 \right] d\psi d\xi. \quad (\text{A.5})$$

Therefore,

$$\sin \phi = \eta_1 \eta_2 \int_z^L \int_\xi^L \int_\xi^L \left[ w_1 \left( 1 - \frac{\psi}{L} \right) - w' \cos \phi_1 \right] d\psi d\xi d\zeta. \quad (\text{A.6})$$

Equations (A.3) and (A.6) are for analysing the deflection of part AC. Because of the non-linearity involved, they should be solved by an iteration method using the following formulae:

$$(w')^{(i+1)} = \int_z^1 \frac{\sin \varphi^{(i)}}{\cos \varphi^{(i)}} d\xi, \tag{A.7}$$

$$\sin \varphi^{(i+1)} = (L')^3 \eta_1 \eta_2 \int_x^1 \int_\zeta^1 \int_\xi^1 \left[ \frac{w_1^{(i)}}{L} (L - L'\psi) - (w')^{(i)} \cos \phi_1 \right] d\psi d\xi d\zeta. \tag{A.8}$$

A.3. The calculation of deflection ignoring the deformation of part AC

When the effect of deformation of cantilever beam is ignored, according to eqns (5) and (25),

$$\frac{d\varphi}{dz} = \frac{\eta_1 m}{\cos \varphi} = \frac{\eta_2 \eta_1 w_1}{6L \cos \varphi} (L - z)^3, \tag{A.9}$$

$$\sin \varphi = \lambda \left( 1 - \left( 1 - \frac{z}{L} \right)^4 \right), \quad \lambda = \sin \varphi_c = \frac{\eta_1 \eta_2}{24} L^3 w_1, \tag{A.10}$$

where  $\varphi_c$  is the slope of the cantilever beam at end C, see Fig. 2(c). Let

$$\frac{z}{L} = 1 - \sqrt[4]{1 - \frac{\sin \varphi}{\lambda}},$$

then

$$dz = \frac{L \cos \varphi d\varphi}{4 \sqrt[4]{\lambda(\lambda - \sin \varphi)^3}}. \tag{A.11}$$

The substitution of eqn (A.11) into eqn (A.3) immediately leads to

$$w' = \int_z^L \frac{\sin \varphi}{\cos \varphi} dx = \int_\varphi^{\varphi_c} \frac{L \sin \varphi d\varphi}{4 \sqrt[4]{\lambda(\lambda - \sin \varphi)^3}} = LG_3, \tag{A.12}$$

where

$$G_3 = \int_\varphi^{\varphi_c} \frac{\sin \psi d\psi}{4 \sqrt[4]{\lambda(\lambda - \sin \psi)^3}} \tag{A.13}$$

is an elliptical integration.

A.4. The elliptical integration

A.4.1. The calculation of  $G_1$  and  $G_2$  in eqn (19). If  $\gamma_1 \geq 1$ , then

$$\begin{aligned} G_1 &= \int_0^\theta \left( 1 - \frac{1}{2}k^2 \sin^2 \psi - \frac{1}{8}k^4 \sin^4 \psi - \frac{1}{16}k^6 \sin^6 \psi - \frac{5}{128}k^8 \sin^8 \psi \right) d\psi \\ &= g_1 \theta + g_2 \sin 2\theta + (g_3 - g_6) \sin^3 2\theta + (g_4 - g_7) \sin 4\theta - g_5 \sin 8\theta, \end{aligned} \tag{A.14}$$

$$\begin{aligned} G_2 &= \int_0^\theta \cos \psi \left( 1 - \frac{1}{2}k^2 \sin^2 \psi - \frac{1}{8}k^4 \sin^4 \psi - \frac{1}{16}k^6 \sin^6 \psi - \frac{5}{128}k^8 \sin^8 \psi \right) d\psi \\ &= (\sin \theta - \frac{1}{6}k^2 \sin^3 \theta - \frac{1}{40}k^4 \sin^5 \theta - \frac{1}{112}k^6 \sin^7 \theta - \frac{5}{1152}k^8 \sin^9 \theta), \end{aligned} \tag{A.15}$$

where

$$\begin{aligned} g_1 &= \left[ 1 - \frac{k^2}{4} - \frac{3k^4}{64} - \frac{5k^6}{256} - \frac{175k^8}{1024} \right], & g_2 &= \frac{1}{8} \left( k^2 + \frac{k^4}{4} + \frac{k^6}{8} + \frac{5k^8}{64} \right), \\ g_3 &= \frac{1}{384} (k^6 + \frac{5}{4}k^8), & g_4 &= \frac{1}{256} \left( k^4 + \frac{3k^6}{4} + \frac{35k^8}{64} \right), \\ g_5 &= \frac{5k^8}{131072}, & g_6 &= \frac{k^6}{192}, & g_7 &= \frac{5k^8}{8192}, & k^2 &= 1 - \frac{1}{\gamma_1^2}. \end{aligned} \tag{A.16}$$

If  $\gamma_1 < 1$ , then

$$\begin{aligned} G_1 &= \int_0^\theta \left(1 - \frac{1}{2}k^2 \cos^2 \psi - \frac{1}{8}k^4 \cos^4 \psi - \frac{1}{16}k^6 \cos^6 \psi - \frac{5}{128}k^8 \cos^8 \psi\right) d\psi \\ &= (g_1 \theta - g_2 \sin 2\theta + g_3 \sin^3 2\theta - g_4 \sin 4\theta - g_5 \sin 8\theta), \end{aligned} \quad (\text{A.17})$$

$$\begin{aligned} G_2 &= \int_0^\theta \cos \psi \left(1 - \frac{1}{2}k^2 \cos^2 \psi - \frac{1}{8}k^4 \cos^4 \psi - \frac{1}{16}k^6 \cos^6 \psi - \frac{5}{128}k^8 \cos^8 \psi\right) d\psi \\ &= h_1 \sin \theta - h_2 \sin^3 \theta - h_3 \sin^5 \theta - h_4 \sin^7 \theta - h_5 \sin^9 \theta, \end{aligned} \quad (\text{A.18})$$

where

$$\begin{aligned} h_1 &= \left(1 - \frac{k^2}{2} - \frac{k^4}{8} - \frac{k^6}{16} - \frac{5k^8}{128}\right), \quad h_2 = -\left(\frac{k^2}{2} + \frac{k^4}{4} + \frac{3k^6}{16} + \frac{5k^8}{32}\right), \\ h_3 &= \frac{(8k^4 + 12k^6 + 75k^8)}{2560}, \quad h_4 = \frac{(2k^6 + 5k^8)}{224}, \quad h_5 = \frac{5k^8}{1152}, \quad k^2 = 1 - \gamma_1^2. \end{aligned} \quad (\text{A.19})$$

A.4.2. *The calculation of  $G_2$  in (A.13).* Letting

$$v^4 = \lambda - \sin \varphi, \quad d\varphi = \frac{-4v^3 dv}{\sqrt{1 - (\lambda - v^4)^2}}, \quad 0 \leq v \leq v_1 = \sqrt[4]{\lambda}, \quad (\text{A.20})$$

$G_3$  can be rewritten as

$$G_3 = \int_0^{v_1} \frac{1}{\sqrt[4]{\lambda}} \frac{(\lambda - \xi^4) d\xi}{\sqrt{1 - (\lambda - \xi^4)^2}}. \quad (\text{A.21})$$

Using the Taylor series expansion, it becomes

$$\begin{aligned} G_3 &= \lambda \int_0^{v_1} \frac{(\lambda - \xi^4)}{\sqrt[4]{\lambda}} \left[1 + \frac{1}{2}(\lambda - \xi^4)^2 + \frac{3}{8}(\lambda - \xi^4)^4 + \frac{15}{48}(\lambda - \xi^4)^6 + \frac{105}{384}(\lambda - \xi^4)^8 + \dots\right] d\xi \\ &= [g_1 \lambda + \frac{1}{2}g_2 \lambda^3 + \frac{3}{8}g_3 \lambda^5 + \frac{15}{48}g_4 \lambda^7 + \dots], \end{aligned} \quad (\text{A.22})$$

where

$$\begin{aligned} g_1 &= \int_0^{v_1} (1 - u^4) du, \quad g_2 = \int_0^{v_1} (1 - u^4)^3 du, \quad g_3 = \int_0^{v_1} (1 - u^4)^5 du, \\ g_4 &= \int_0^{v_1} (1 - u^4)^7 du, \quad u = \left(1 - \frac{x}{\alpha L}\right). \end{aligned} \quad (\text{A.23})$$